

Fracture mapping in challenging environment: a 3D virtual reality approach combining terrestrial LiDAR and high definition images

G. Mastrorocco¹  · R. Salvini¹ · C. Vanneschi²

Received: 5 July 2016 / Accepted: 2 March 2017 / Published online: 10 March 2017
© Springer-Verlag Berlin Heidelberg 2017

Abstract The latest technological developments in computer vision allow the creation of georeferenced, non-immersive desktop virtual reality (VR) environments. VR uses a computer to produce a simulated three-dimensional world in which it is possible to interact with objects and derive metric and thematic data. In this context, modern geomatic tools enable the remote acquisition of information that can be used to produce georeferenced high-definition 3D models: these can be used to create a VR in support of rock mass data processing, analysis, and interpretation. Data from laser scanning and high quality images were combined to map deterministically and characterise discontinuities with the aim of creating accurate rock mass models. Discontinuities were compared with data from traditional engineering-geological surveys in order to check the level of accuracy in terms of the attitude of individual joints and sets. The quality of data collected through geomatic surveys and field measurements in two marble quarries of the Apuan Alps (Italy) was very satisfactory. Some fundamental geotechnical indices (e.g. joint roughness, alteration, opening, moisture, and infill) were also included in the VR models. Data were grouped, analysed, and shared in a single repository for VR visualization and stability analysis in order to study the interaction between geology and human activities.

Keywords Fracture mapping · Terrestrial LiDAR · High definition digital photos · Virtual reality · Marble quarries

Introduction

A rock mass is a natural system composed of intact rock separated by a fracture network (Brady and Brown 1994; Goodman 1989) that can influence the physical–mechanical behaviour of the whole rock structure. Discontinuities, including joints, bedding planes, faults, and other types of fractures, can provide preferential pathways for the circulation of fluids and represent surfaces of weakness and alteration that lead to block and wedge failures. Discontinuities also affect local stress orientation and magnitude. Different disciplines, such as civil engineering, engineering geology (e.g. mining and dam stability), petroleum geology, and hydrogeology, therefore, require a deep understanding of rock mass structures, including detailed knowledge of fracture patterns.

Modern geomatic techniques can lend support to traditional engineering-geological surveys in the characterization of rock masses. This approach enables deterministic fracture mapping, even in inaccessible and critical areas, using manual or semi-automatic techniques. Different methods, such as terrestrial laser scanning (TLS), close-range imaging, and instruments such as total stations (TS) and global positioning system (GPS) receivers can be used together to acquire remote data. In this context, the engineering-geological community commonly uses light detection and ranging (LiDAR) for landslide monitoring and, more recently, for rock outcrop characterization, rockfall hazard assessment and 3D structural and stratigraphic modelling (Assali et al. 2014; Bellian et al. 2005; Buckley et al. 2008; Deliormanli et al. 2014; Fekete et al.

✉ G. Mastrorocco
giannim87@gmail.com

¹ Department of Environment, Earth and Physical Sciences and Centre of GeoTechnologies CGT, University of Siena, Via Vetri Vecchi 34, 52027 San Giovanni Valdarno, AR, Italy

² Camborne School of Mines, College of Engineering, Mathematics and Physical Sciences, University of Exeter, Penryn, Cornwall TR10 9FE, UK

2010; Francioni et al. 2014, 2015; Kemeny et al. 2006; Pejic 2013; Slob et al. 2005; Strouth and Eberhardt 2005; Sturzenegger and Stead 2009; Sturzenegger et al. 2011; Vanneschi et al. 2014).

This study tested the use of TLS, integrated with high definition digital photos, in characterizing rock masses at two marble quarries in the Apuan Alps (Tuscany, Italy). The TLS point clouds, georeferenced through a topographic survey carried out using GPS and TS, were used to map fracture surfaces in the laboratory and to measure their geometric characteristics, grouping them into discontinuity sets. The importance of the study lies in the fact that fractures may intersect rock faces, causing instability and affecting the yield of extractable raw materials. Discontinuity detection and characterization is not always possible through the use of point clouds (sometimes even when the spatial resolution is very high) especially in flat artificial quarry walls. As an alternative, fracture traces can be measured using optical imaging methods (Maerz and Otoo 2014) associating high definition (HD) images with TLS point clouds. This approach allowed, in the present work, the creation of very detailed and realistic 3D rock mass models that can be shown in a freeware panoramic VR such as LeicaTM TruView to determine the geometric characteristics of discontinuities. The presented approach takes advantage of VR, which thanks to computer vision, duplicates the ability of humans to perceive and understand an image (Jähne and Haußecker 2000). The aim was to create a free, compact and easy to use virtual repository of high-resolution panoramic images (360° wide) and associated LiDAR data to which it is possible to add structural information (from fracture mapping) and traditional engineering-geological data from fieldwork.

This paper describes two case studies: the first is an underground marble quarry called “Romana”, in which a freeware VR code was used to map and measure discontinuities and to present and store their geomechanical properties; the second is an open pit called “Orto di Donna”, in which in addition to the approach described above, fracture surfaces were also detected using TLS point clouds.

Methodology

Rock mass discontinuities generally crop out as fracture surfaces or fracture traces: the former are three-dimensional geometrical elements, whereas the latter are two-dimensional elements representing the intersection between fractures and the outcrop face. Surfaces can be detected and measured using LiDAR data, whereas traces can be better mapped in VR after matching HD images and

point clouds (e.g. from LiDAR, UAV—unmanned aerial vehicle). Point data without HD photographs, unless at very high spatial resolution, are difficult to manage and interpret: these data do not allow detailed observations or easy identification and understanding of traces for attitude calculation. Note that the walls of marble pits are usually very flat, especially within the underground quarry. Given the need to analyse fracture traces for slope stability studies, this work tested a specific approach for locating discontinuities and measuring their orientation. Measurements were performed not only on point clouds and using the digital surface model (the standard procedure in open pits or natural slopes—Abellàn et al. 2014; Fanti et al. 2013; Salvini et al. 2013), but also taking advantage of HD photos and freeware plug-in for VR visualization and mapping.

This methodology for 3D data visualization, processing, and analysis has many advantages over traditional hand mapping techniques in reconstructing the morphological setting of a rock mass. For example, the geometry, attitude, and spacing of joints and the volume of blocks measured during fieldwork are often inaccurate due to lack of data and compass deviations; moreover, this classical approach is time-consuming and limited by safe access to outcrops (Assali et al. 2014; Deliormanli et al. 2014; Fekete et al. 2010). In this context, the plug-in gives free access to data; it can be used to represent and control both LiDAR and RGB data and, more importantly, to measure joints by extracting 3D strings or arrays of aligned georeferenced points.

Geomatics strategy

Laser scanning

LiDAR is a remote sensing technology that uses a laser beam (with wavelength varying between the visible and near infrared portion of the spectrum—532 nm in this work) to measure the distance between a source point and a reflective surface so as to create a 3D point cloud of surfaces and objects that fall within the field of view of the scanner.

In order to create realistic surface models, the absolute xyz coordinates of the point clouds, the reflectance (reflectivity) of surfaces and RGB data from the associated photographic images were collected.

Different types of laser scanners for a wide variety of applications are available on the market. They differ, for example, for acquisition method and speed, accuracy, and distance range. Laser scanners can also help in the interpretation process by allowing the classification of acquired data in terms of roughness or surface reflectance (full waveform laser scanners—Hartzell et al.

2013). They can be used in either dynamic mode, on ships, UAV and aircrafts, or in static mode, using terrestrial platforms.

From a technical point of view, the laser scanner measures a time period between two events according to two time-based scanning principles: pulse-based (time-of-flight) or phase-based. In the first type, the system measures the time a laser pulse takes to travel from a source to a reflective surface and back again (round trip); once the time is known, given that the velocity is equal to the speed of light, it is possible to calculate the distance between the source and the target. The working principle of the second type is based on the modulation in amplitude of the emitted (incoherent) light; the scattered reflection from a surface is collected and the system measures the phase difference between the sent and received waveforms, hence the delay time. Typical phase-based scanners modulate their signal using sinusoidal modulation, amplitude-based (AM) or frequency-based (FM) modulation, pseudo-noise or polarization modulation (Lerma García et al. 2008; Vosselman and Hans-Gerd 2010).

In this study, the LiDAR survey was carried out using a pulse-based static terrestrial laser scanner. The instrument has 360° horizontal and 270° vertical fields of view and must be firmly mounted on a tripod. In order to observe the surrounding environment as completely as possible and to reduce shadows, LiDAR data are generally acquired from several different scan positions (Lato et al. 2010). TLS produces a raw point cloud in an *xyz* coordinate system, which is relative to the scanner optical centre. LiDAR data are usually used in conjunction with topographic data (GPS and TS) in order to link scan data to an absolute coordinate system (georeferencing). TS provides millimetric accuracy of the origin of the laser scanner and of a reference 0-Azimuth direction (Beshr and Elnaga 2011; Vanneschi et al. 2014). This accuracy can also be achieved for optical high reflectivity targets positioned in different and strategic places within the scanned area. The registration process consists of a 3D linear roto-translation of the TS data, which can be accomplished using the absolute coordinates of the origin and its reference 0-Azimuth direction (also measured by GPS receivers), so that the targets are identified in the selected reference system with millimetric accuracy. After topographic data processing, the targets are used to constrain the system and align the scans (registration) and to georeference them to an absolute system. At the end of this process, the final georeferenced point cloud can be edited so that all irrelevant objects acquired during the scans are removed (Fig. 1a).

The characteristics of geomatic instruments used in this work are summarised in Table 1.

Close-range imaging

Close-range imaging is a technique that can be used to create high-resolution photo-mosaics to be matched with LiDAR point clouds in order to produce 3D photorealistic models suitable for photo-interpretation. High resolution images were obtained in this work by replacing the laser scanner on the top of the tripod, with a digital camera properly fitted on a special bracket and positioned on the terrestrial laser scanner tribrach. This substitution was carefully made without moving the tripod and the laser scanner blister (Fig. 1b). In order to acquire a panoramic image (360° view—Fig. 1c), photos were shot at preset angles with sufficient overlap with reference to the selected focal length (Table 2); for example, a fish eye lens can be used to shoot only six photos (every 60°), whereas a different optical system with smaller preset camera aperture angles requires a greater number of photos.

The correct alignment of HD photos to TLS point clouds (texture mapping) is possible when the focal centre of the camera lens matches the optical centre of the scanner (Leica Geosystems 2015a). In the laboratory, photos were processed using specific software for the creation of equirectangular images (PTGui™—New House Internet Services BV). After conversion to Cube Maps images using Pano2QTVR Gui (Garden Gnome software™—Fig. 1d), photographs were aligned to the LiDAR data (Fig. 1e—Leica™ Cyclone) and ready to be published in Leica™ TruView.

Desktop virtual reality

Leica™ TruView is a plug-in that allows the visualization of 3D VR and can be run within Microsoft™ Internet Explorer. The dataset is created from the alignment of high resolution images to LiDAR data and can represent any VR, including natural slopes, rock cuts and discontinuities, with very high 3D geometric resolution in a compact format. In particular, this panoramic viewer allows to navigate from every laser scanner position through virtual environments and to interact in a non-immersive desktop VR. By using the Markup and Hotlinks options, this plug-in also allows one to measure distances and to extract 3D real coordinates (Fig. 2) that may be used to locate, identify and represent discontinuities: each click into the VR view corresponds to a point of the cloud with respective coordinates that can be saved and exported.

Computer algorithm for dataset information extraction

The code for 3D VR visualization allows users to extract information from the dataset through extensible markup language files (*.xml format). Given the complexity and

GEOMATICS STRATEGY

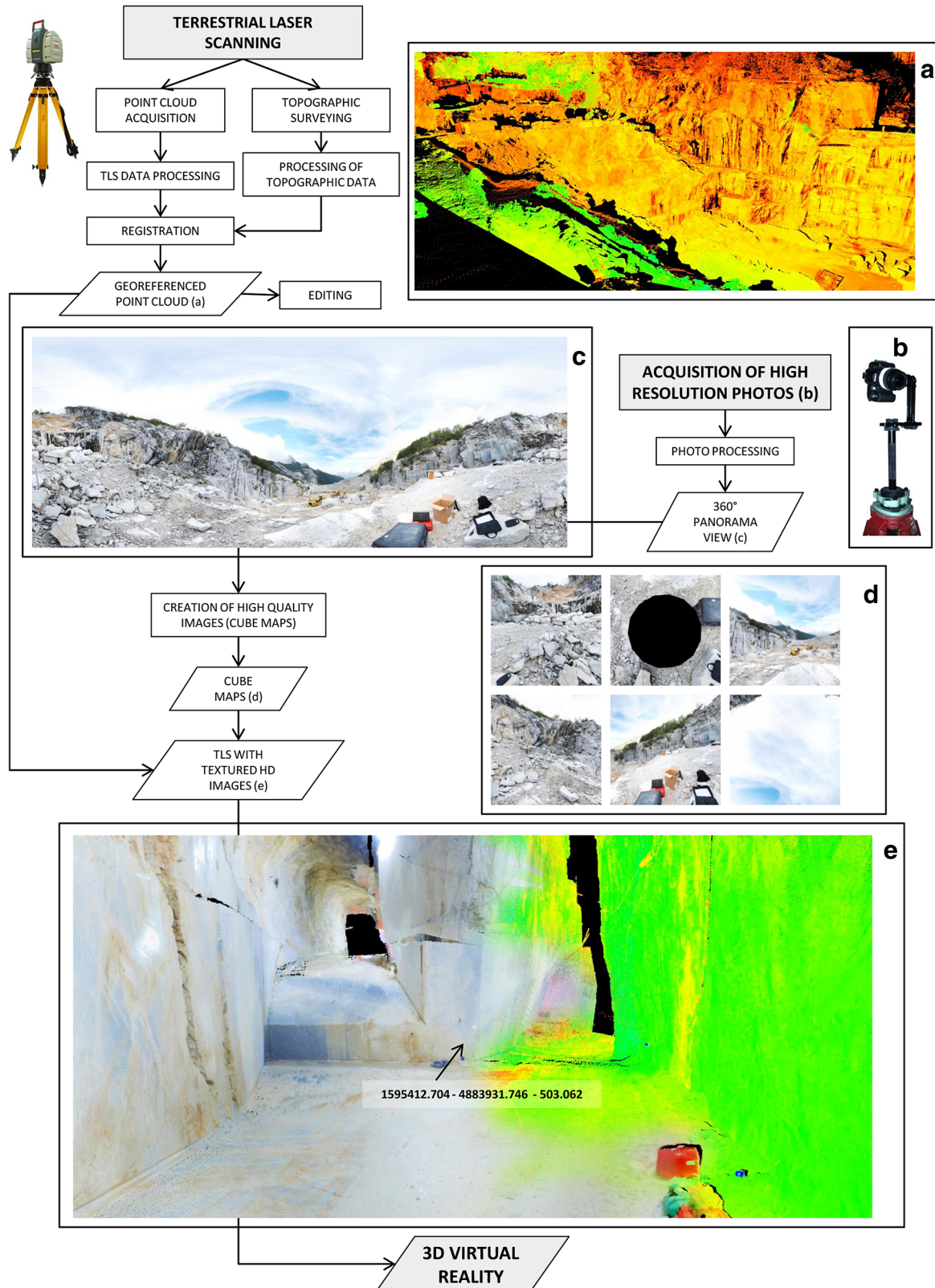


Fig. 1 Workflow of the geomatic strategy used to support 3D computer vision. **a** TLS with georeferenced point cloud. **b** Acquisition of high resolution photos. **c** 360° panoramic view. **d** Creation of HD images (Cube Maps). **e** TLS with textured HD images

Table 1 Instrument characteristics

Terrestrial laser scanner		Leica™ ScanStation 2
Instrument type		Pulsed
Scan rate		Up to 50,000 points/s
Field of view	Horizontal	360° (max)
	Vertical	270° (max)
Accuracy of single measurement	Position	6 mm (at 50 m range, one sigma)
	Distance	4 mm (at 50 m range, one sigma)
Scan resolution	Spot size	From 0–50 m to 4–6 mm
	Maximum sample density	<1 mm
Target acquisition		2 mm std. deviation
GPS receivers		#2 Leica™ Viva System 1200
		Dual-frequency
Total station (Romana quarry)		Leica™ TCRP 1205 + R1000
Angle measurement	Hz and V accuracy	5" (1.5 mgon)
Distance measurement	Prism	1.5 m to 3000
	Non-prism	1.5 m to 1000
Laser dot size		at 30 m 7 mm × 10 mm at 50 m 8 mm × 20 mm
Total station (Orto di Donna quarry)		MultiStation Leica™ Nova MS50
Angle measurement	Hz and V accuracy	1" (0.3 mgon)
Distance measurement	Prism	1.5 m to >10,000 m
	Non-prism	1.5 m to 2000 m
Laser dot size		at 50 m 8 mm × 20 mm

Table 2 Characteristics of the camera used during the Romana and Orto di Donna surveys and acquisition strategy

Camera	Nikon™ D80
Lens	Nikon™ AF-S Nikkor 18–55 mm
Focal length	18 mm
Diaphragm aperture	f/8
Bracket	Leica™ Nodal Ninja 3II
Vertical acquisition angles	–12°, 25° and 62°
Horizontal acquisition angle	25.7°
Image number	42

quantity of information contained in a single *.xml file related to point and linear data measured on the quarry walls, the geomatic dataset was processed using an algorithm especially created by the authors in Microsoft™ Visual Basic Standard (Fig. 3). The program requires a textual file (input), represented by a self-describing data formats, created on the 3D VR and containing the following info: (1) View Name, (2) Mark Pos, and (3) Text. The “View Name” string represents the number of the panoramic view that includes a fracture trace; the “Mark Pos” string refers to the 3D coordinates of aligned points (Markup) of a fracture trace; the “Text” string is specifically created to integrate engineering-geological information from fieldwork. After the “Markup.xml” file is

uploaded, the algorithm creates a table, called “Fracture”, used to store the information contained into the above described strings. The operating environment used to perform the instructions is automatically created. The program prompts the user to insert the scan number by displaying the created button and generates a temporary output file. Using the first loop, the algorithm scans the text and searches the string “View Name”; at the second loop it searches the string “Mark Pos” in order to collect the Markup 3D coordinates from LiDAR data; successively, the algorithm creates an output file which includes the xyz coordinates, the view name and the scan number through a structured query language (SQL) code (i.e. “Append Values”). When the aforementioned loops are not verified the code searches the string “Text” and writes it into the output file. The final output of the process is represented by an ASCII file containing xyz coordinates and IDs (label, view, and scan number) for each joint.

Based on the geomatic data it was possible to compute the dip and dip direction of fractures using the Leica™ Cyclone code as described in the following section. Furthermore, integration of geomatics and engineering-geological data allowed the creation of a new spatial dataset comprising high resolution panoramic images complemented by structural and geomechanical information. This information was copied into the *.xml file as explained into the case studies section.

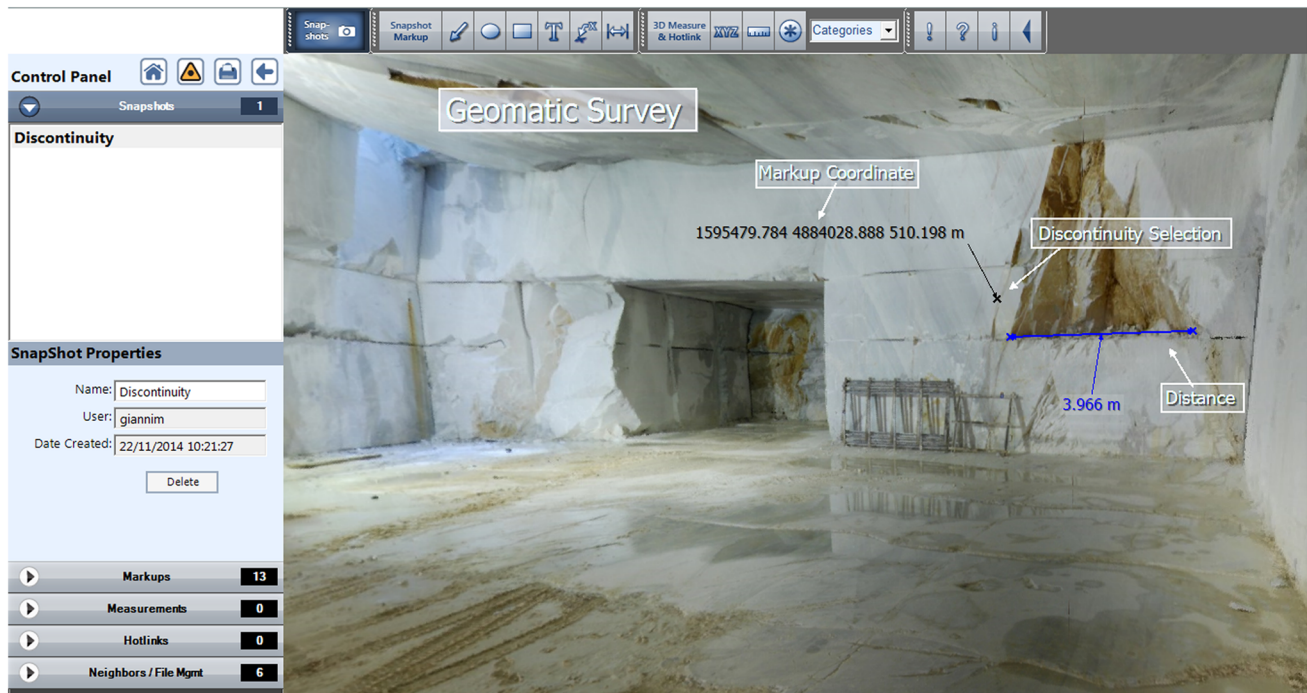


Fig. 2 3D VR window and tools used to identify discontinuities

Computation of joint attitude from the geomatic dataset

In this work authors used LeicaTM Cyclone, a specific software for point cloud management, editing, and analysis to determine the attitude of fractures mapped in the VR code and processed as ASCII files. The software was also used to map additional rock mass fractures directly on the 3D point clouds and to artificially model the fractures by means of several coplanar points. In fact, in order to compute the attitude of joint traces two alignments of points coplanar with the surface under investigation are necessary (joint traces consisting of a single line are excluded from the computation). On the other hand, when the joint surface is fully visible, a minimum of three points is required to identify the plane. Given that only one plane passes through three points in space, trigonometric Eqs. (1) and (2) were used to estimate the dip direction (α) and dip (β) of joints using spatial vector components u_x , u_y , and u_z (Francioni et al. 2014; Priest 1993). The following equations were adopted:

$$\alpha = \arctan\left(\frac{u_x}{u_y}\right) + q, \quad (1)$$

$$\beta = \arctan\left[\frac{u_z}{\sqrt{(u_x^2 + u_y^2)}}\right]. \quad (2)$$

The q parameter is an angle between 0° and 360° which ensures that α lies in the correct quadrant. Considering that

the arctan function yields results ranging between -90° and $+90^\circ$, the q angle must assume the following values:

$$\begin{aligned} q &= 0^\circ \text{ for } u_x \geq 0 \text{ and } u_y \geq 0; \\ q &= 180^\circ \text{ for } u_x < 0 \text{ and } u_y \geq 0; \\ q &= 180^\circ \text{ for } u_x < 0 \text{ and } u_y < 0; \\ q &= 360^\circ \text{ for } u_x \geq 0 \text{ and } u_y < 0. \end{aligned}$$

Case study

Romana quarry

The Romana underground marble quarry is located in the Province of Massa (Tuscany) and comprises a network of interconnected tunnels with a total length of about 600 m (Fig. 4).

From a geological point of view, the quarry is located in the polydeformed Apuan Alps metamorphic complex. In particular, it lies within the “Monte Rasori” antiform (Carmignani et al. 1993), a geological fold structure located on the inverted limb of the “Orto di Donna” syncline. The marble varieties cropping out belong to the group of white marbles, veined marbles and dolomitic marbles (Carmignani et al. 2007; Vanneschi et al. 2014).

The geo-structural study of the rock mass was carried out by combining terrestrial LiDAR data with engineering-geological surveys. The spatial analysis of point clouds and image data in the VR plug-in enabled the measurement of the attitude, persistence and spacing of joints. Traditional

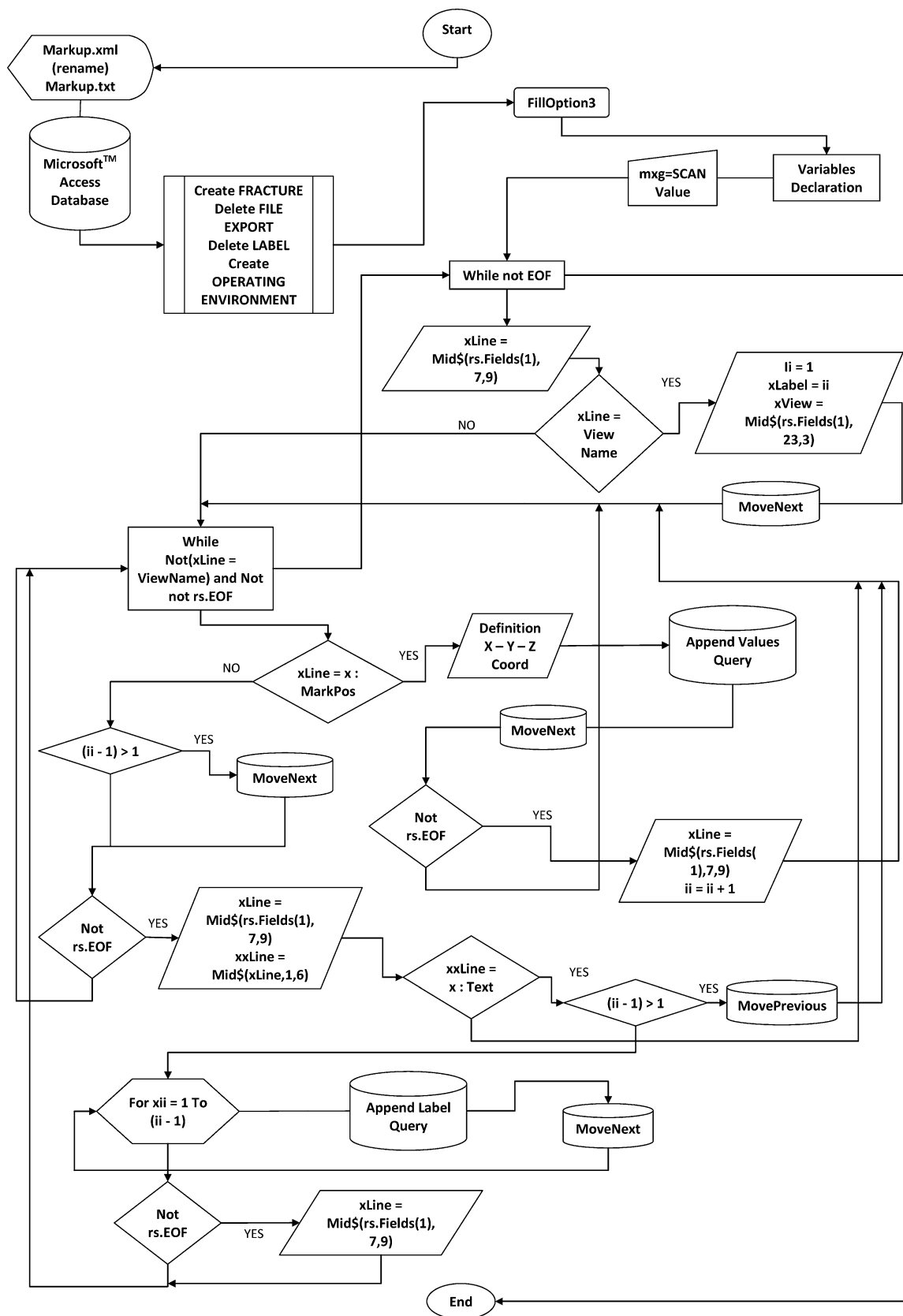


Fig. 3 Flowchart describing the algorithm created by the authors in Microsoft™ Visual Basic Standard

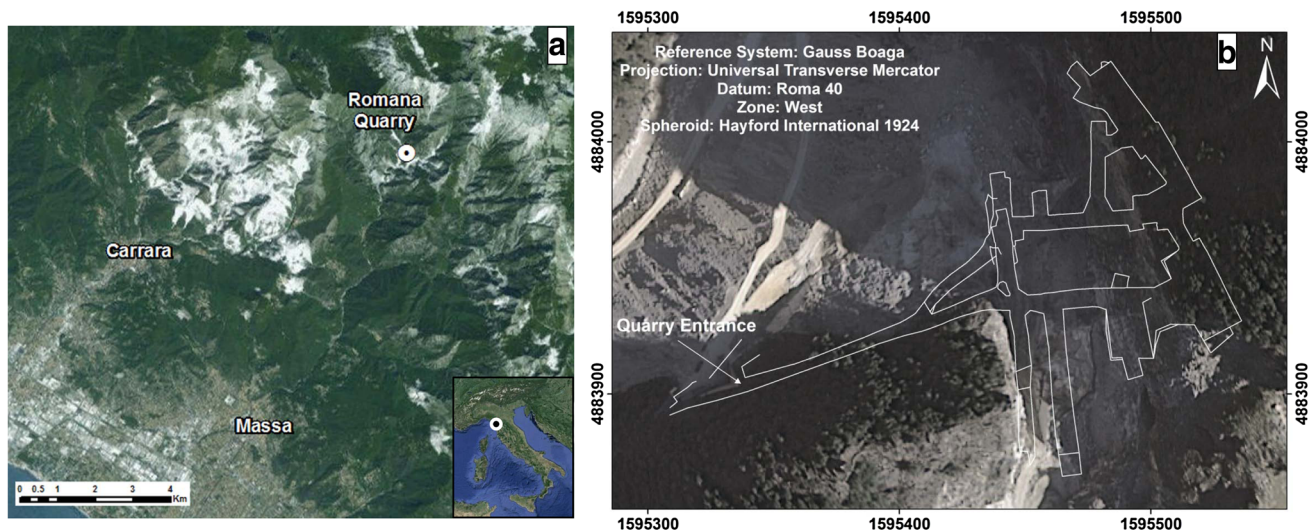


Fig. 4 **a** Satellite image of the Apuan Alps; *inset* map shows the location of the quarry, in Italy. **b** Aerial orthophoto and planimetry of the underground quarry

fieldwork data was used to identify and assess discontinuities and to determine other fundamental mechanical fracture properties. The accuracy of the geomatic data was assessed through comparison with data from the traditional engineering-geological survey (using a geological compass in accessible areas) by means of stereographic projections. Lastly, integration of geomatic and engineering-geological data permitted the creation of a new spatial dataset that comprises high-resolution 3D images, LiDAR data, and geo-structural mechanical information.

Dataset strategy

The geomatic dataset is characterised by 12 different scans (the first scan corresponds to the service area outside the underground quarry) containing a variable numbers of 3D views and georeferenced markups with associated IDs (labels). Markups can be used to measure and represent traces of discontinuities. Each view contains only one fracture such that the scan number and view number refer to a single fracture with associated markups and labels (Fig. 5).

Engineering-geological survey

The geomatic study, undertaken to support fracture mapping, was used to determine the engineering-geological characteristics of discontinuities. Despite the ease with which joint persistence and spacing can be measured, the method cannot be used to collect other fundamental mechanical properties necessary for a complete understanding of rock mass behaviour; in particular, indices such as roughness (JRC—Joint Roughness

Coefficient—Barton 1973), alteration, joint wall compressive strength (JCS—Joint Compressive Strength—Deere and Miller 1966), opening, infill, termination, and seepage cannot be derived from the geomatic data. Nevertheless, the engineering-geological survey benefited from fracture mapping directly into the 3D VR software and allowed the integration of geomechanical characteristics and the identification of additional joints within the quarry. During fieldwork, the dataset from VR mapping was consulted in order to use the same IDs for discontinuities, to assess their attitude, and to integrate information.

Fracture mapping results

The TLS survey conducted in the Romana quarry, the characteristics of which are shown in Table 3, was used to map a total of 710 points, corresponding to 150 discontinuities, by means of VR.

The data was statistically analysed using RocscienceTM Dips software to identify possible local distributions and determine the main discontinuity sets (Table 4). Figure 6a and b illustrate the stereographic projection of discontinuities measured respectively in VR and using a geological compass during a traditional engineering-geological survey (Schmidt equal-area representation method, lower hemisphere). Comparison between dip and dip direction reveals an angular difference from 1° to 11° between the two sets of data (Table 4).

As an example of comparison between single fracture plans, Fig. 7 shows a fault trace with a calculated (VR) attitude of 16°/87° and a measured (geological compass) attitude of 10°/85°.

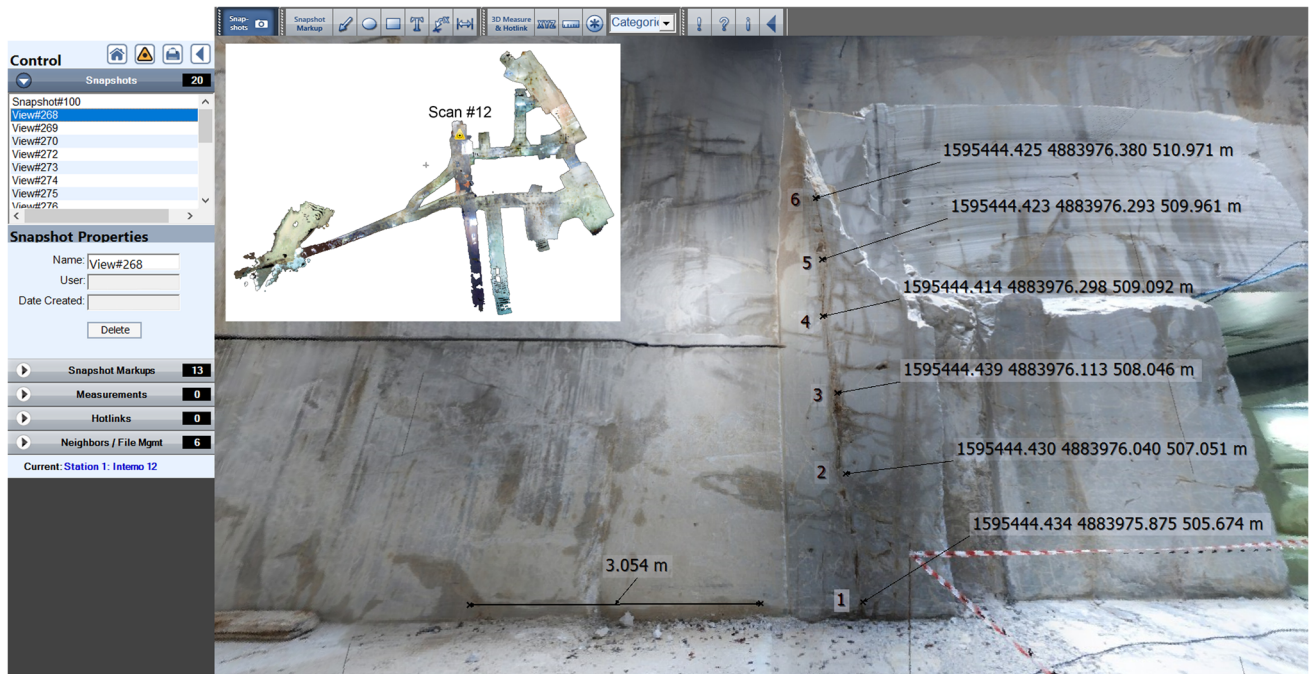


Fig. 5 Example of fracture mapping using markups with associated IDs and georeferenced 3D coordinates. In this example, the fracture is identified by the scan number (Scan 12), the view number (View#268) and some markups with relative coordinates and labels

Table 3 Characteristics of the TLS survey at the Romana quarry

	Romana quarry
Executed scans#	13
Plano-altimetric accuracy (registration)	4 mm (average)
Point cloud density	1.2 cm (at 10 m range)
Targets used for registration#	60
GPS\TS processing software	Leica™ Geo Office
TS\TLS processing software	Leica™ Cyclone

Integration of geomatics and engineering-geological data allowed the creation of a new spatial dataset comprising high-resolution panoramic images complemented by structural and geomechanical information. This was easily achieved by typing engineering-geological information directly into the VR plug-in. As an alternative, information can be copied into the *.xml file following the <cx:Text> command (Fig. 8). An example of such integration is shown in Fig. 9, where it is possible to

observe the properties of the major fracture on a pillar. The same approach can be adopted for all the mapped fractures, providing a powerful, easy to use and compact tool for engineering-geological studies.

Orto di Donna quarry

The Orto di Donna quarry is located in the Province of Lucca (Tuscany) and presents a planar “U” shape. The two elongated fronts are oriented approximately NNW-SSE and have a total length of about 300 m (the westernmost one) and 150 m (the easternmost one— Fig. 10).

From a geological standpoint, the quarry is located on the inverted limb of the “Orto di Donna” syncline and presents many marble varieties: homogeneous dark grey marbles, white marbles with thin grey veins and zones with alternating white marbles and light grey marbles with evident dolomitic beds (Carmignani et al. 2007; Coli et al. 1987). Rock cuts are characterised by benches 4–15 m high

Table 4 Characteristics of joint systems in the Romana quarry as obtained from VR and from the engineering-geological survey

Set	Dip\dip direction mean value (VR)		Dip\dip direction standard deviation (VR)		Dip\dip direction mean value (field measurement)		Dip\dip direction standard deviation (field measurement)		Difference between dip\dip direction mean values	
K1a/b	86/268	86/90	2.49/5.15	3.84/5.50	83/265	85/81	4.39/9.87	3.81/6.17	3/3	1/9
K2a/b	81/188	85/1	0.71/4.35	2.58/3.78	86/199	80/8	1.22/4.88	8.33/7.96	5/11	5/7
K3a/b	85/144	85/332	2.82/3.71	3.05/3.78	84/143	86/326	4.02/9.85	2.71/14.80	1/1	1/6

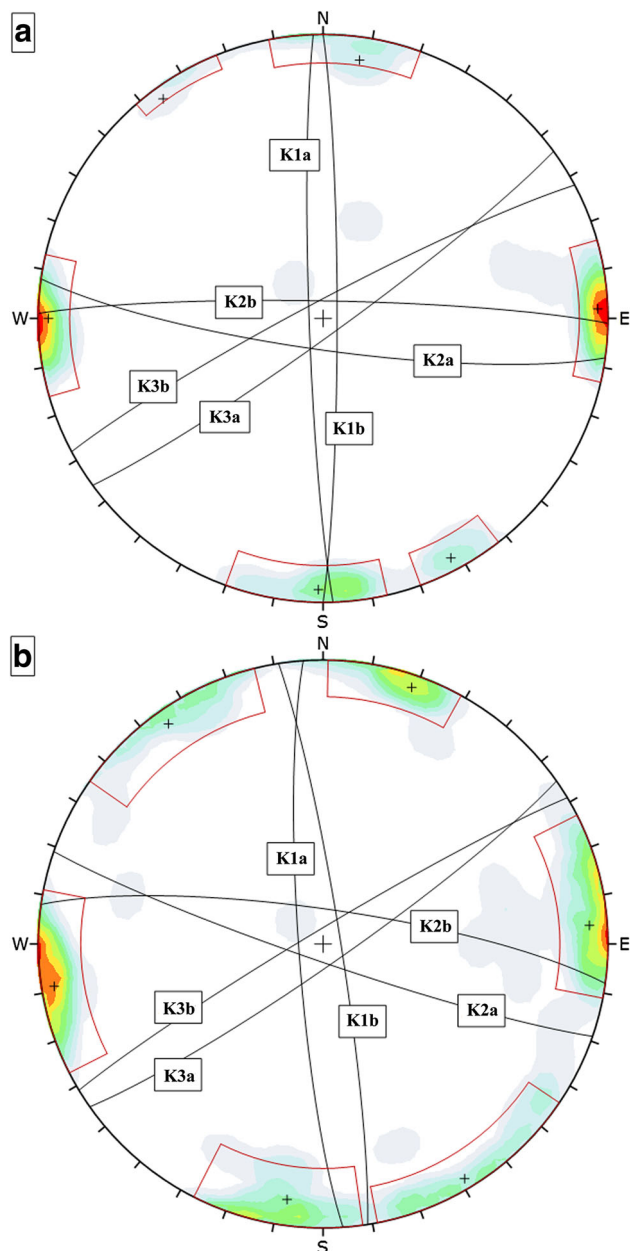


Fig. 6 **a** Stereographic representation of discontinuities at the Romana quarry measured using VR. **b** Stereographic representation derived from a traditional engineering-geological survey. Schmidt equal-area method, lower hemisphere

with fractures that differ in length from tens of meters to decimeters and penetrate to depths difficult to assess (frequently more than 1 m). The intersection of discontinuities with natural and artificial rock slopes is critical in determining the behaviour of rock wedges and blocks that are sometimes subject to gravitational instability, such the 2013 event (Fig. 11).

Geometric and structural studies were carried out using terrestrial LiDAR data and HD photos in order to map and analyse discontinuities in the Orto di Donna quarry and to

identify and characterize potentially unstable blocks deriving from previous extraction activities.

Engineering-geological survey

Engineering-geological analysis was carried out along with the geomatic survey in order to measure and characterize the geometric and mechanical properties of joints. A total of five scanline surveys were executed in safe, accessible areas, and scattered measurements were taken at rock cuts and outcrops. Measurements include the attitude (dip and dip direction), roughness, alteration, joint wall compressive strength, opening, infill, termination, and seepage of each fracture.

Fracture mapping results

Fracture planes and potentially unstable blocks were identified by visual photointerpretation using both TLS point clouds and HD images processed with PTGui and Pano2QTVR Gui. Table 5 shows the characteristics of the TLS survey at Orto di Donna quarry. As described earlier, discontinuity mapping was done by selecting several coplanar points in the point clouds in Cyclone and HD images in the VR plug-in. In this way, the normal components of each surface were used to compute the dip direction and dip of the fractures using Eqs. 1 and 2. A total of 948 fractures were mapped in this way.

In order to represent the spatial distribution of discontinuities and to identify the principal discontinuity sets, the statistical distribution of fracture poles was determined using stereographic representations. Figure 12a and b illustrate the projections of discontinuity poles measured through geomatics and traditional engineering-geological surveys, respectively. The two sets of data were then compared in order to assess the accuracy of the geomatic survey (Table 6). Comparison between the dip and dip direction of joint sets in this case revealed angular differences from 0° to 12° .

Dataset representation

VR was used to illustrate the interpreted data and extract additional information from the georeferenced LiDAR and HD scenes. The created markups show the position and attitude of the main discontinuities that were classified into the sets shown in Table 6.

A preliminary kinematic stability analysis revealed that the most evident rocky blocks and wedges are potentially unstable: these were represented using markups and hotlinks to high resolution images showing their location and size (volume in m^3 —Fig. 13a, b). Kinematic stability analysis was performed using slope and joint attitudes from

Fig. 7 Example of fault trace, the attitude of which was used to assess the reliability of single measurements by photointerpretation in VR; perspective view, the scale bar is only indicative



the geomatic surveys and the friction angle from the engineering-geological survey.

Discussion

Results from the presented case studies highlight advantages and limitations of the presented methodology. As LeicaTM TruView uses a storage mechanism (“Patent Pending”) consisting of digital images for visualization and an encoded representation of scan points, the proposed approach is not affected by errors due to the creation of a geomatic dataset. Each dataset contains scan and image data relative to a single TLS location. The code is image-based and stores at most one scan point per image pixel, since the user would have no way of identifying different scan points if they occurred in the same pixel. As a result, smaller images hold fewer scan

points than larger ones; because the dataset contains fewer points than the original scan, it is easier to use (Leica Geosystems 2015b). Moreover, measurements through 3D VR do not contain errors that can affect data collected through traditional mapping surveys (e.g. approximations in geological compass positioning, difficulties in inspecting inaccessible areas, safety concerns under the excavation walls). In contrast, the VR code generates an error, called an E_{ENCODING} error, due to its compact dataset. As a result, points are slightly shifted with respect to their original location. Another source of error (E_{SCANNER}) is related to the horizontal and vertical accuracy of the adopted laser scanner (section “Geomatics strategy”). The total error in the dataset is thus a combination of E_{ENCODING} and E_{SCANNER} errors as a function of range. Table 7 shows the total error (E_{TOTAL}) of points stored in the dataset. Furthermore, a millimetric error due to the registration of different point clouds


```

    <cx:Brush Color="#f0f0ff" Transparency="0.878"/>
    <cx:Position>957.2866 375.4795</cx:Position>
    <cx:Text>2</cx:Text></cx:TextMark>
    <cx:TextMark FontSize="12.000" FontName="Tahoma">
    <cx:Created>07/05/2013 16.36.25</cx:Created>
    <cx:User>giannim</cx:User>
    <cx:Pen Color="#00ff00" Transparency="0.000"
width="2.000" Dash="0.000"/>
    <cx:Brush Color="#f0f0ff" Transparency="0.878"/>
    <cx:Position>837.7018 304.3977</cx:Position>
    <cx:Text>3</cx:Text></cx:TextMark>
    <cx:TextMark FontSize="12.000" FontName="Tahoma">
    <cx:Created>14/08/2013 16.54.46</cx:Created>
    <cx:User>Enzo</cx:User>
    <cx:Pen Color="#00ff00" Transparency="0.000"
width="2.000" Dash="0.000"/>
    <cx:Brush Color="#f0f0ff" Transparency="0.878"/>
    <cx:Position>463.0000 295.0000</cx:Position>
    <cx:Text>- Type : Joint
Dip_Direction : 252°
Dip : 54°
Length : >10(m)
Persistence : >10(cm/m)
Opening : 1(cm)
Roughness : 4-8
Ending : x-x
Filing : Soft
R_(M.Schmidt)_Rock : 50
R_(M.Schmidt)_Disc. : 40
water : wet
</cx:Text></cx:TextMark></cx:Marks></cx:View>
<cx:View Name="View#145" GUID="{8A8FCE3A-94BF-4E85-8FDB-58FCCF897749}">

```

Fig. 8 Example of an *.xml file with engineering-geological information added (indicated by the rectangle)

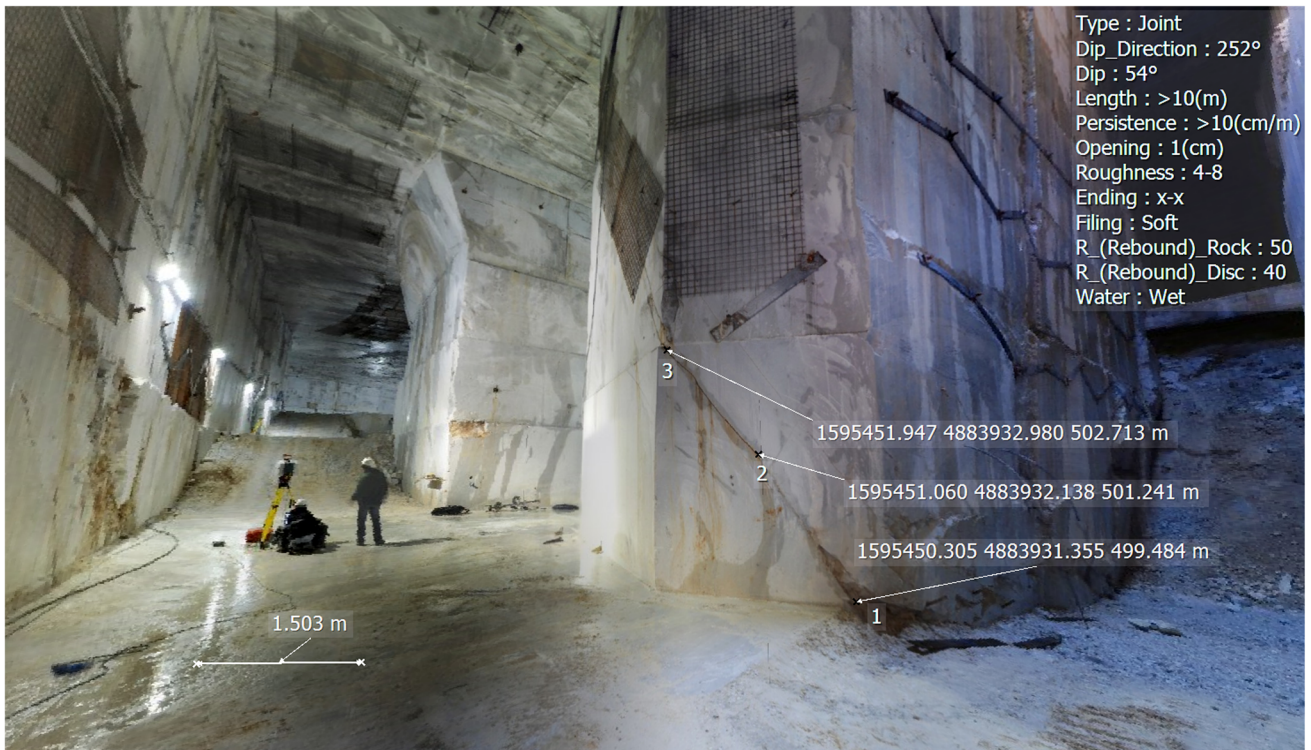


Fig. 9 Example of a VR window; on the upper right, following the Bieniawski classification (Bieniawski 1989), the text shows the engineering-geological characteristics of the discontinuity displayed

on the bottom right through markup, coordinates and IDs; given that this is a perspective view, the distance indicated at the bottom left is only indicative (modified from Salvini et al. 2014)

recorded from different positions must be added to the total error. In this study, considering the millimetric error due to the registration process and the scan distance

range (max 200 m), the sum of errors can be considered negligible in fracture mapping, but could possibly affect attitude measurements.

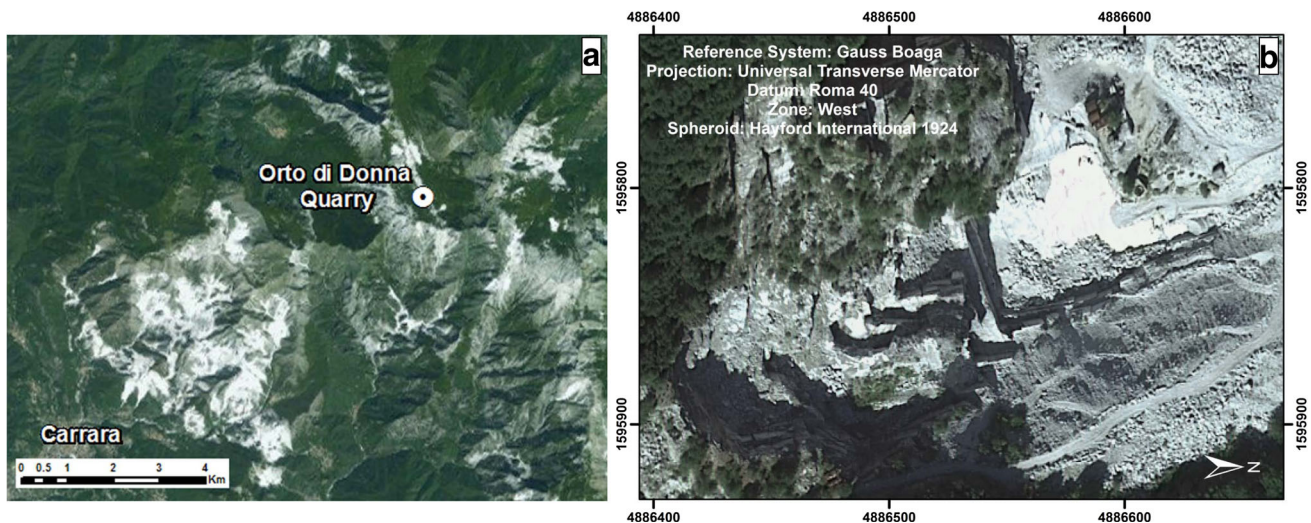


Fig. 10 **a** Satellite image of the Apuan Alps and location of the Orto di Donna quarry. **b** Aerial orthophoto of the open pit

Fig. 11 Panoramic view of the rock fall that occurred at Orto di Donna quarry in 2013. Dashed line indicates the detachment zone; continuous line indicates the depositional zone



In any case, this was not a problem for the two test sites as demonstrated in sections “Fracture mapping results”. Another limitation of the used plug-in is that fracture mapping is possible only for joint traces observed on at least two surfaces. This is because it is impossible to model a surface using a single line of points. This was a problem in the case of the artificial smooth cuts within the underground quarry. For this reason, other software such as 3DM Analyst Mine Mapping Suite (ADAM TechnologyTM) or alternative methods (Kemeny and Post 2002; Maerz and Otoo 2014) that can overcome this problem are currently

being tested. Several papers have shown the use and reliability of automatic and semi-automatic procedures that can be adopted in fracture mapping based on images and point clouds (Assali et al. 2014; Gigli and Casagli 2011; Lato et al. 2009; Lato and Voge 2012; Mah et al. 2011; Riquelme et al. 2014; Slob et al. 2005; Vasuki et al. 2014; Voge et al. 2013). Although different automatic software such as TerranumTM Coltop 3D, Split-FXTM, CloudCompareTM, and MaptrekTM I-Site Studio have been tested by the authors (Forzini 2014; Salvini 2014), in this work we adopted a fully manual approach in order to guarantee the

Table 5 Characteristics of the TLS survey at the Orto di Donna quarry

	Orto di Donna quarry
Executed scans#	4
Plano-altimetric accuracy (registration)	4 mm (average)
Point cloud density	0.5 cm (at 10 m range)
Targets used for registration#	18
GPS\TS processing software	Leica™ Geo Office
TS\TLS processing software	Leica™ Cyclone

consistency and high quality of interpreted discontinuities, as well as having complete process control. In our experience, the automatic mapping reliability and validity depends on software calibration and, especially, morphology of quarry faces. Furthermore, different results can be achieved when using a 3D point cloud or a model (i.e. mesh) in automated identification of geological structures; within some software the mesh reconstruction can represent a tricky issue that can cause a local loss of accuracy due to the point density, presence of shadows and interpolation method.

In this work, the adopted manual approach was particularly suited because Apuan Alps quarries are usually characterized by smooth cut surfaces where only traces of discontinuities are visible; this means that automatic identification of geological structures resulted to be useless in the selection process. Additionally, the presence of local blasting areas can create unnatural surfaces that increase errors and uncertainties in the discontinuity characterisation. In order properly to use an automatic software, it is also necessary to isolate rock mass portions that are constituted only by natural fractures or to select natural discontinuities by the automatic models. Both these approaches can be more time consuming than the manual selection. Authors retain that a manual deterministic fracture mapping increases the level of control of the process and it is essential in these particular case studies. Note that in the first case study the flat morphology of quarry walls was such that it was only possible to identify the traces, not the planes, of discontinuities. In the second, the quarry slopes are characterised by numerous blasting areas that create ambiguity in the discontinuity characterisation. In conclusion, a final visual inspection of outputs is always required, even when using codes for the automatic identification of joints.

Conclusions

This work describes the methodology that was used to create two large 3D virtual repositories of geological-structural and geomechanical information, TLS point

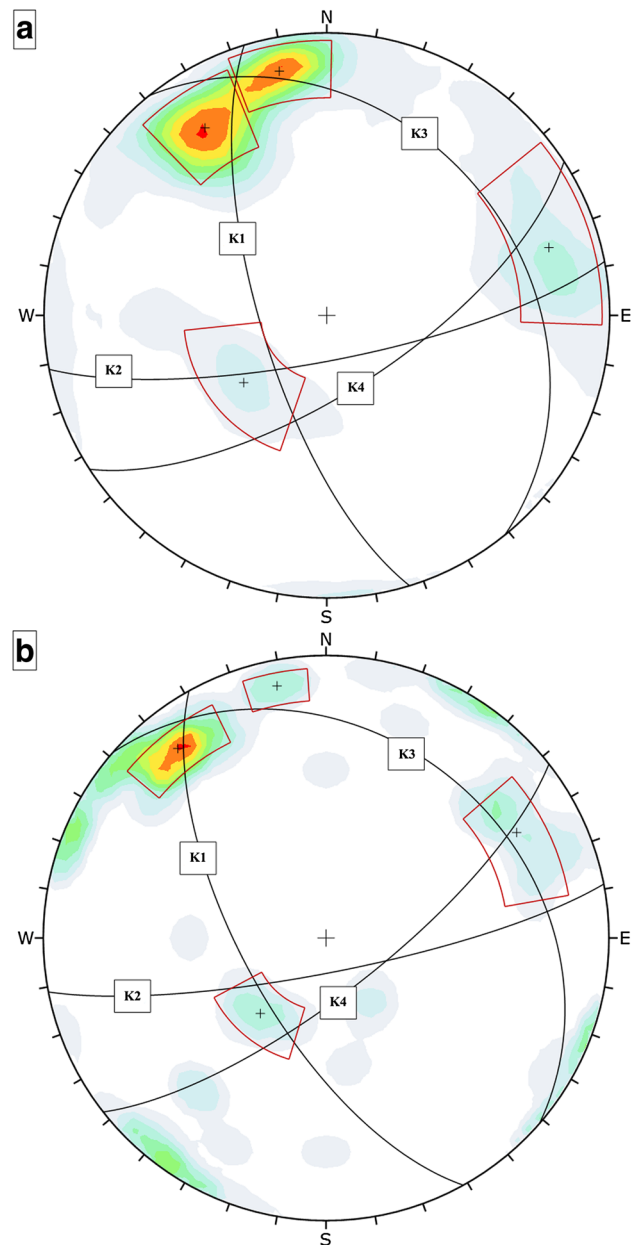


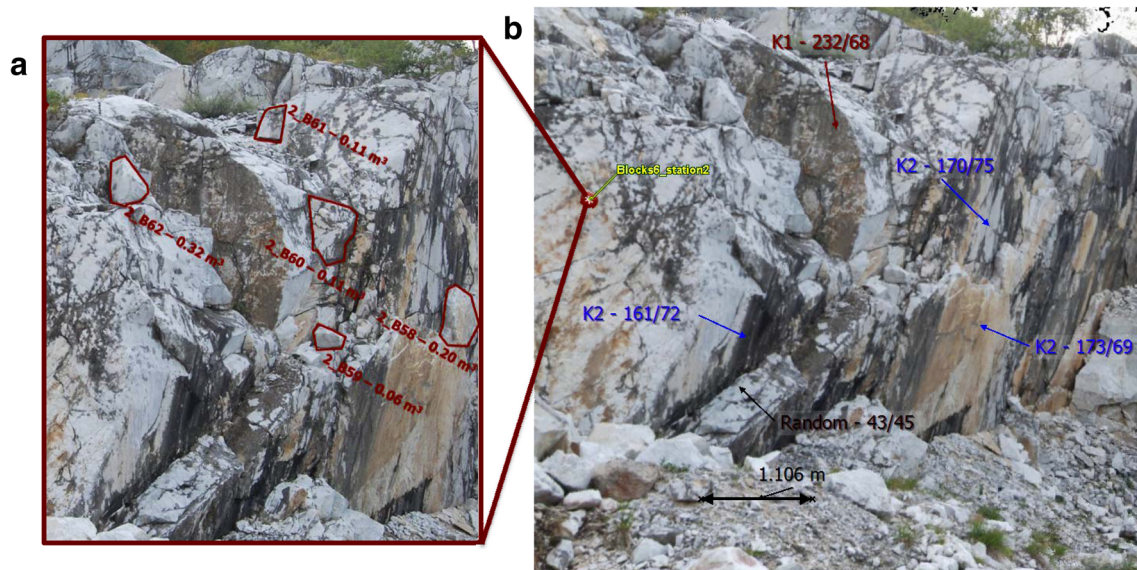
Fig. 12 **a** Stereographic representation of discontinuities measured at the Orto di Donna quarry using geomatic techniques. **b** Stereographic representation derived from a traditional engineering-geological survey; Schmidt equal-area method, lower hemisphere

clouds, and high-resolution panoramic images (360° view). The 3D visualization, post-processing and analysis of data were carried out using a free plug-in.

At the Romana quarry, fracture mapping based on both geomatics and engineering-geological surveys allowed the identification of three discontinuity sets. Comparison of results revealed high consistency between traditional in situ measurements and interactive virtual mapping of LiDAR data using VR.

Table 6 Characteristics of joint systems at the Orto di Donna quarry; data was collected using geomatic techniques and through the engineering-geological survey

Set	Dip\dip direction mean value (VR-TLS)	Dip\dip direction standard deviation (VR-TLS)	Dip\dip direction mean value (field measurement)	Dip\dip direction standard deviation (field measurement)	Difference between dip\dip direction mean values
K1	71/253	7.39/6.36	66/241	3.91/6.02	5/12
K2	77/169	5.02/5.96	80/169	0.57/1.00	3/0
K3	31/51	5.67/17.90	29/41	5.99/11.23	2/10
K4	68/147	7.70/12.04	74/142	3.76/14.96	6/5

**Fig. 13** a Example of image used as a hotlink to potentially unstable blocks. b Example of a VR panoramic view with markups and hotlinks**Table 7** Leica™ TruView errors in image-to-point alignment at different ranges (Leica Geosystems 2015b)

Range (m)	E _{SCANNER} (mm)	E _{ENCODING} (mm)	E _{TOTAL} (mm)
200	17	6	23
100	9	3	12
50	6	2	7
10	4	1	5

Four sets of discontinuities were identified at the Orto di Donna quarry. The interpretation of point clouds and HD images was again in good agreement with data collected through traditional structural mapping. In particular, stereographic projections of fracture poles at the Orto di Donna quarry reveal that discontinuities identified through virtual mapping have greater dispersion than the ones identified through in situ fieldwork; this is probably in relation to previous blasting and cutting activities.

In this context, geomatics, when used in synergy with traditional techniques, is an effective tool for studying rock masses and performing stability analyses. Large quantities of data obtained from different sources are often scattered in datasets with differing characteristics. Such data is therefore difficult to manage within one environment. The consultation and analysis of data (even by third parties) such as HD photos, point clouds, geological and structural maps, and geomechanical sheets usually requires different, sometimes expensive software. The presented method allows the compression of point clouds that could easily reach several gigabytes in size, making data handling easier. In this context, the use of a single tool can greatly simplify data processing/management and accessibility. Data can be grouped, accessed, analysed and shared within a single repository, where a software able to contain diverse geomatic information and a georeferenced 3D VR, can be used to complete detailed structural discontinuity mapping and rock mass characterization by using the simple computer algorithm specifically created and

illustrated in this paper. This provides a powerful, easy to use and compact tool for engineering-geological studies.

In conclusion, the proposed procedure should not be considered an alternative to traditional in situ surveys but a complementary tool for analysing data. Indeed, fieldwork is still required to derive the fundamental geomechanical properties of individual discontinuities such as compressive strength, narrow aperture, infill, and alteration. Despite the huge technological advancements in geology, classical survey methods are therefore still important to ensure safety and profit in mining.

Acknowledgements The authors gratefully acknowledge the assistance of the personal of the Romana Quarry and particularly Corniani M. This paper was possible because of support from the Tuscany Region Research Project known as “Health and safety in the quarries of ornamental stones—SECURECAVE”. The authors acknowledge Pellegri M and Gulli D (Local Sanitary Agency n.1, Mining Engineering Operative Unit—Department of Prevention) and Riccucci S (Centre of GeoTechnologies, University of Siena) for their support of this research.

References

- Abellàn A, Oppikofer T, Jaboyedoff M, Rosser NJ, Lim M, Lato MJ (2014) Terrestrial laser scanning of rock slope instabilities. *Earth Surf Proc Land* 39:80–97
- Assali P, Grussenmeyer P, Villemin T, Pollet N (2014) Surveying and modeling of rock discontinuities by terrestrial laser scanning and photogrammetry: semi-automatic approaches for linear outcrop inspection. *J Struct Geol* 66:102–114
- Barton NR (1973) Review of a new shear strength criterion for rock joints. *Eng Geol* 7:287–332
- Bellian JA, Kerans C, Jennette DC (2005) Digital outcrop models: applications of terrestrial scanning lidar technology in stratigraphic modeling. *J Sediment Res* 75(2):166–176
- Beshr AAA, Elnaga IMA (2011) Investigating the accuracy of digital levels and reflectorless total stations for purposes of geodetic engineering. *Alex Eng J* 50:399–405
- Bieniawski ZT (1989) *Engineering rock mass classifications*. Wiley, New York, p 272
- Brady BHC, Brown ET (1994) *Rock mechanics for underground mining*. Chapman & Hall, London, p 571
- Buckley S, Howell J, Enge H, Kurz T (2008) Terrestrial laser scanning in geology: data acquisition, processing and accuracy considerations. *J Geol Soc* 165(3):625–638
- Carmignani L, Fantozzi PL, Giglia G, Meccheri M (1993) Pieghe associate alla distensione duttile del complesso metamorfico apuano. *Mem Soc Geol Italiana* 49:99–124
- Carmignani L, Conti P, Fantozzi PL, Mancini S, Massa G, Molli G, Vaselli L (2007) I marmi delle Alpi Apuane. *Geitalia* 21:19–30
- Coli M, Grandini G, Matteini L (1987) *Carta Strutturale del bacino marmifero di Orto di Donna (Alpi Apuane), 1:5000*. SELCA, Firenze
- Deere DUR, Miller P (1966) Engineering classification and index properties for intact rock. Technical Report AFNL-TR-65-116, National Technical Information Service, Air Force Weapons Laboratory, New Mexico, pp 300
- Deliormanli AH, Maerz NH, Otoo J (2014) Using terrestrial 3D laser scanning and optical methods to determine orientations of discontinuities at a granite quarry. *Int J Rock Mech Min* 66:41–48
- Fanti R, Gigli G, Lombardi L, Tapete D, Canuti P (2013) Terrestrial laser scanning for rockfall stability analysis in the cultural heritage site of Pitigliano (Italy). *Landslides* 10(4):409–420
- Fekete S, Diederichs M, Lato M (2010) Geotechnical and operational applications for 3-dimensional laser scanning in drill and blast tunnels. *Tunn Undergr Space Technol* 25:614–628
- Forzini C (2014) *Analisi della fratturazione nei versanti in roccia a partire da dati laser scanner terrestre. Sperimentazione di differenti software per l'estrazione semi-automatica dei dati di giacitura*. Dissertation, University of Siena
- Francioni M, Salvini R, Stead D, Litrico S (2014) A case study integrating remote sensing and distinct element analysis to quarry slope stability assessment in the Monte Altissimo area, Italy. *Eng Geol* 183:290–302
- Francioni M, Salvini R, Stead D, Giovannini R, Riccucci S, Vanneschi C, Gulli D (2015) An integrated remote sensing-GIS approach for the analysis of an open pit in the Carrara marble district, Italy: slope stability assessment through kinematic and numerical methods. *Comput Geosci* 67:46–63
- Gigli G, Casagli N (2011) Semi-automatic extraction of rock mass structural data from high resolution LIDAR point clouds. *Int J Rock Mech Min* 48:187–198
- Goodman RE (1989) *Introduction to rock mechanics*, 2nd edn. Wiley, New York, p 562
- Hartzell PJ, Glennie CL, Finnegan DC (2013) Calibration of a terrestrial full waveform laser scanner. In: *Conference American Society of Photogrammetry and Remote Sensing (ASPRS)*, Baltimore, Maryland, p 7
- Jähne B, Haußbeck H (2000) *Computer vision and applications: a guide for students and practitioners*. Academic Press, New York, p 679
- Kemeny J, Post R (2002) Estimating three-dimensional rock discontinuity orientation from digital images of fracture traces. *Comput Geosci* 29:65–77
- Kemeny J, Turner K, Norton B (2006) LIDAR for rock mass characterization: hardware, software, accuracy and best-practices. In: Tonon F, Kottenstette JT (eds) *Proceedings of the Laser and Photogrammetric Methods for Rock Face Characterization*, American Rock Mechanics Association, Alexandria, pp 49–62
- Lato MJ, Voge M (2012) Automated mapping of rock discontinuities in 3D lidar and photogrammetry models. *Int J Rock Mech Min Sci* 54:150–158
- Lato M, Diederichs MS, Hutchinson DJ, Harrap R (2009) Optimization of LiDAR scanning and processing for automated structural evaluation of discontinuities in rockmasses. *Int J Rock Mech Min* 46:194–199
- Lato M, Diederichs MS, Hutchinson DJ (2010) Bias correction for static LiDAR scanning of rock outcrops for structural characterization. *Rock Mech Rock Eng* 23:615–628
- Leica Geosystems (2015a) Cyclone external camera workflow-Nodal Ninja bracket. <http://scansw.leica-geosystems.com/public/camera/>. Accessed 03 February 2015
- Leica Geosystems (2015b) Leica TruView Accuracy. http://leica-geosystems.com/downloads/123/hds/general/cyclone/white-tech-paper/Leica_Trueview_Accuracy_us.pdf. Accessed 25 March 2015
- Lerma García JL, Van Genechten B, Heine E, Santana Quintero M (2008) *Theory and practice on Terrestrial Laser Scanning*. Editorial de la Universidad Politécnica de Valencia, Valencia, p 261
- Maerz NH, Otoo JN (2014) Integrating discontinuity trace and facet orientation measurements for improved discontinuity data analysis. *Int J Rock Mech Min Sci* 72:300–303

- Mah J, Samson C, McKinnon SD (2011) 3D laser imaging for joint orientation analysis. *Int J Rock Mech Min Sci* 48:932–941
- Pejic M (2013) Design and optimisation of laser scanning for tunnels geometry inspection. *Tunn Undergr Space Technol* 37:199–206
- Priest SD (1993) Discontinuity analysis for rock engineering. Chapman and Hall, London, p 473
- Riquelme AJ, Abellán A, Tomás R, Jaboyedoff M (2014) A new approach for semi-automatic rock mass joints recognition from 3D point clouds. *Comput Geosci* 68:38–52
- Salvini R (2014) Developments in UAV and LiDAR technology, data acquisition and processing. In: Stead D, Elmo D (eds) Short course on data collection for discrete fracture networks, 1st International conference on discrete fracture network engineering, Vancouver, British Columbia, Canada, p 55
- Salvini R, Francioni M, Riccucci S, Bonciani F, Callegari I (2013) Photogrammetry and laser scanning for analyzing slope stability and rock fall runout along the Domodossola-Iselle railway, the Italian Alps. *Geomorphology* 185:110–122
- Salvini R, Mastrococco G, Vanneschi C, Riccucci S, Francioni M, Stead D (2014) Excavation stability analysis in an underground marble quarry in the Apuan Alps (Italy): application of terrestrial LIDAR, conventional methods and numerical modeling. In: Kennard D, Stead D, Eberhardt E, Elmo D (eds) Proceedings of the 1st international conference on discrete fracture network engineering, Vancouver, October 19–22, p 11
- Slob S, Van Knapen B, Hack R, Turner K, Kemeny J (2005) Method for automated discontinuity analysis of rock slopes with three-dimensional laser scanning. *Transp Res Rec* 1913:187–194
- Strouth A, Eberhardt E (2005) The use of LIDAR to overcome rock slope hazard data collection challenges at Afternoon Creek, Washington. In: Proceedings of the 41st US Symposium on Rock Mechanics, American Rock Mechanics Association, Golden, Colorado, June 17–21, p 12
- Sturzenegger M, Stead D (2009) Close-range terrestrial digital photogrammetry and terrestrial laser scanning for discontinuity characterization on rock cuts. *Eng Geol* 103:163–182
- Sturzenegger M, Stead D, Elmo D (2011) Terrestrial remote sensing-based estimation of mean trace length, trace intensity and block size/shape. *Eng Geol* 119:96–111
- Vanneschi C, Salvini R, Massa G, Riccucci S, Borsani A (2014) Geological 3D modeling for excavation activity in an underground marble quarry in the Apuan Alps (Italy). *Comput Geosci* 69:41–45
- Vasuki Y, Holden EJ, Kovesi P, Micklethwaite S (2014) Semi-automatic mapping of geological Structures Using UAV-based photogrammetric data: an image analysis approach. *Comput Geosci* 69:22–32
- Voge M, Lato MJ, Diederichs MS (2013) Automated rockmass discontinuity mapping from 3-dimensional surface data. *Eng Geol* 164:155–162
- Vosselman G, Hans-Gerd M (2010) Airborne and terrestrial laser scanning. Whittles Publishing, Dunbeath